ROYAL SOCIETY OF CHEMISTRY

PAPER

Check for updates

Identity of the local and macroscopic dynamic elastic responses in supercooled 1-propanol†

Peter Weigl, ✴[ab] Tina Hecksher, ✴[c] Jeppe C. Dyre, [c] Thomas Walther [b] and Thomas Blochowicz [a]

Glass-forming liquids are well known to have significant dynamic heterogeneities, leading to spatially grossly varying elastic properties throughout the system. In this paper, we compare the local elastic response of supercooled 1-propanol monitored by triplet state solvation dynamics to the macroscopic dynamic shear modulus measured by a piezo-electric gauge. The time-dependent responses are found to be identical, which means that the dynamic macroscopic shear modulus provides a good measure of the average local elastic properties. Since the macroscopic shear modulus of a dynamically inhomogeneous system in general is not just the average of the local moduli, there was no reason to expect such a result. This surprising finding not only provides constraints for models of dynamical heterogeneities in glass-forming liquids, but also allows for a fairly straightforward check on elastic models for glassy dynamics.

1 Introduction

The study of viscous liquids and the glass transition is an age-old field of inquiry.[1–6] A more recent realization is that the physics of a highly viscous liquid approaching the glass transition is dominated by dynamic (not to be mixed with structural) heterogeneities in the sample.[7–11] Thus, the sudden molecular rearrangements termed "flow events" that take place throughout the liquid do not occur (dynamically) homogeneously. Instead, there are places of significant activity and places of little activity. After some time the activity "hotspots" move to different locations.

In many ways, a supercooled liquid behaves like an amorphous solid that flows.[12] Simulation studies of amorphous solids show important spatial variations of, for instance, the local elastic constants.[13–20] Thus, one expects the local elastic response of a highly viscous liquid to vary spatially. Unfortunately, few techniques are able to probe the local elastic response. A promising method is triplet state solvation dynamics (TSD) pioneered by Richert.[21] This method is based

on the fact that dye molecules dissolved in the solvent under investigation induce a local disturbance when photo excited. This initiates reorientation dynamics of the solvent molecules in the first solvation shell, leading to a Stokes shift of the phosphorescence spectrum. TSD monitors this Stokes shift in a time-resolved experiment. The locality of the TSD method originates from the fact that approximately the first solvation shell around a dye molecule is affected, *i.e.* roughly a single molecular layer of solvent molecules, in the order of 1 nm or even below.

While it is well established that the local response function of dipolar phosphorescence dyes is comparable to the macroscopic dielectric signature of the α and β relaxations,[22–26] the situation for nonpolar dyes is less straightforward.[26,27] Although it was found for nonpolar fluorescence dyes at higher temperatures ($T \gg T_g$) that the local response function is comparable to a local shear relaxation,[28,29] this has to our knowledge not yet been evidenced in the long-time and low-temperature regime of TSD. For fluorescence dyes a viscoelastic continuum model describes this kind of local shear relaxation and fits the data quite well.[28–31] This model is based on the fact that the volume of the nonpolar dye changes upon excitation, which results in shear forces acting on the solvent molecules, initiating a relaxation process taking the system back to equilibrium.[31] In the case of naphthalene, the origin of these local shear forces would be the expansion of the molecule known from *ab initio* simulations upon excitation into the triplet state.[32,33]

Recent theories for viscous liquid dynamics assume a distribution of local elastic properties and calculate the overall,

[a] *Institute for Condensed Matter Physics, Technical University of Darmstadt, 64289 Darmstadt, Germany. E-mail: peter.weigl@physik.tu-darmstadt.de*

[b] *Institute for Applied Physics, Technical University of Darmstadt, 64289 Darmstadt, Germany*

[c] *Glass & Time, IMFUFA, Dept. of Science and Environment, Roskilde University, DK-4000 Roskilde, Denmark. E-mail: tihe@ruc.dk*

† Electronic supplementary information (ESI) available: These contain details of the fit model of the shear modulus data and how the temperatures of the shear modulus data were interpolated to compare these data with the TSD data at the same temperatures. In addition, Fig. 3 is shown there in a different form of presentation. See DOI: 10.1039/d1cp02671b

This journal is © the Owner Societies 2021

Phys. Chem. Chem. Phys., 2021, **23**, 16537–16541 | **16537**

macroscopic dynamic shear response from this.[17,34] Such theories are difficult to test because of the challenge of measuring the *local* elastic response, even in a spatially averaged version. The aim of the present paper is to fill this gap by comparing the local dynamic elastic response probed by TSD using the nonpolar dye naphthalene (for 1-propanol) to macroscopic dynamic shear modulus data. We find identical responses within the experimental uncertainty. This means that the macroscopic dynamic shear modulus faithfully represents the average local shear responses, at least for 1-propanol.

It may sound obvious that the overall shear elastic modulus of an dynamically inhomogeneous material is simply the average of the local shear moduli, but this is generally the case only when small variations are involved.[35] For significant spatial variations the overall modulus is affected little by soft spots because the overall rigidity is controlled by a percolating structure of hard material;[36] in this case, a simple arithmetic average of the local moduli gives a quite wrong result. This applies both for static and dynamic moduli. Present-day standard methods for calculating the overall elastic response of a (dynamically) inhomogeneous medium (like the effective-medium approximation for media with spatially randomly varying elastic properties[35,36]) take this effect into account. The fact of relevance here, however, is that the overall dynamic shear modulus is generally *not* identical to the average of the local dynamic shear moduli.[17]

The substance under study here, the glass-forming liquid 1-propanol, is a monohydroxy alcohol. The anomalies of these alcohols and their pronounced tendency to form hydrogen-bonded clusters[37,38] make them an obvious choice for testing whether the local average and macroscopic mechanical response are identical. The presence of meso-scale structures in the liquid could well result in quite different local and global mechanical properties, similar to the differences observed between the local dipolar solvation and the macroscopic dielectric response in these materials.[26]

2 Experimental section

The 1-propanol sample was obtained from Alfa Aesar (99.9% purity). Prior to use, the liquid was cleaned for at least 24 hours with a 3 Å molecular sieve and filtered with a 200 nm syringe filter. The nonpolar phosphorescene chromophore naphthalene (NA) was purchased from Sigma Aldrich (99%) and used as received. For TSD experiments the solute/solvent ratio was 1×10^{-4} mol mol^{-1}.

The TSD measurements were performed with the setup described in detail in ref. 26, 39 and 40. In brief: in an optical contact gas cryostat (Conti Spectro 4 from CryoVac), the sample under investigation is located in a quartz glass cuvette. To excite different dye molecules, a pulsed 10 Hz laser system with an integrated pulse divider (based on a Spitlight 600 Nd:YAG laser from Innolas) generates three different UV excitation wavelengths (355, 320, and 266 nm). Under 90° to the incident laser beam, the emitted phosphorescence of the dye molecules is collected by a liquid light guide fiber (model 77566 from Newport) and guided to the entrance slit of a Czerny–Turner grating spectrograph (Shamrock 500i from Andor Technology) equipped with gratings of 150, 600, and 1800 lines per mm, respectively. To detect the dispersed phosphorescence emission, an iCCD camera (iStar 340T from Andor) with integrated gate and delay generator is used.

The phosphorophore naphthalene used here was excited with ~ 2 mJ UV laser pulses of wavelength 266 nm. The repetition rate of the laser was $f_{laser} = 1/8$ Hz $\leq 1/(3\tau_{NA})$, where τ_{NA} is the phosphorescence life time of naphthalene. With increasing temperature τ_{NA} decreases about 20% within 20 K, starting at $\tau_{NA} = (2.56 \pm 0.02)$ s for $T \leq T_{g,cal} = 96$ K. The solvation measurements were performed with a time resolution of $\Delta t/t \leq 8\%$ by using a 600 lines per mm grating. Each spectrum consists of at least 2×10^6 counts at the peak maximum with the background subtracted. By following the common practice[21,26] the high-energy wings of the spectra were fitted to Gaussian functions to obtain the mean energy $\langle \nu \rangle \equiv \nu$ as a function of time and temperature. The long-time limit of the Stokes shift $\nu(\infty)$ was determined by time averaging points at high temperatures where the solvent is entirely relaxed. Analogously, the short-time limit of the Stokes shift $\nu(0)$ was calculated at low temperatures where the solvent is completely unrelaxed. Thus, the absolute Stokes shift $\Delta\nu_{NA} = \nu(0) - \nu(\infty) = (60.9 \pm 2.2)$ cm^{-1} can be evaluated, which is similar to a result published earlier.[27] The shift is only about 10% compared with the dipolar case,[26,27] which illustrates why it is more challenging to generate high-quality data with a nonpolar dye. Similar observations were also made in the case of fluorescence dyes, where nonpolar dyes have absolute Stokes shifts of 100–150 cm^{-1} and polar dyes of 1000–3000 cm^{-1}.[29]

The dynamic shear modulus was measured over seven decades of frequency (1 mHz–10 kHz) with a setup based on a three-disc piezo-ceramic shear transducer.[41–44] Compared to conventional rheometers, this techniques is optimized for measurements on stiff systems (1 MPa–10 GPa).[41]

To validate consistent temperature values between the TSD data (Darmstadt) and the shear data (Roskilde), macroscopic dielectric measurements were performed by the Roskilde group in the same cryostat at the same temperatures right after the respective shear-modulus measurement. Comparing these measurements to dielectric data from Darmstadt, which were temperature calibrated with respect to the TSD sample environment, an absolute temperature accuracy better than 0.5 K was achieved.

3 Results and discussion

Fig. 1 presents the Stokes shift response function $\Delta\nu_{Stokes}(t) = \nu(t) - \nu(\infty)$ for the entire dynamic range. The master plot representation reveals two relaxation processes, α and β relaxation. The relaxation strength of the latter is up to 35%, which is the largest value for a TSD measurement reported so far.[21,24,26] The α-relaxation is described by a stretched exponential

16538 | *Phys. Chem. Chem. Phys.*, 2021, **23**, 16537–16541

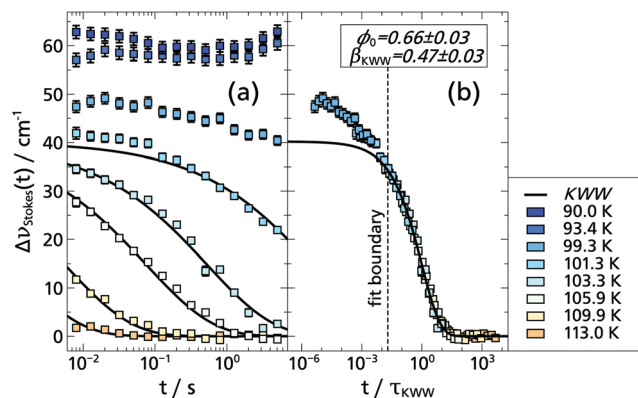This journal is © the Owner Societies 2021

Fig. 1 (a) Stokes shift response functions $\Delta\nu_{\text{Stokes}}(t)$ of naphthalene in 1-propanol. (b) Master plot revealing an α and a β relaxation process. The structural relaxation is fitted by a stretched-exponential function. The data agree with the single curve at $T = 102.3$ K presented in ref. 27.

function, *i.e.*, $\Phi(t) = \Delta\nu_{\text{NA}}\cdot\phi_0\cdot\exp[-(t/\tau_{\text{KWW}})^{\beta_{\text{KWW}}}]$.[21,26] The fit boundary was chosen such that the β process does not affect the fit. The resulting $\beta_{\text{KWW}} \approx 0.5$ is typical for the structural α relaxation observed in TSD experiments[21,22,26,27] and also for nonpolar fluorescence dyes.[28,29]

The imaginary part of the complex dynamic shear modulus $G'(\nu) + iG''(\nu)$ is shown together with suitable fits for eight temperatures in Fig. 2 (upper panel). The fit curves result from an electrical equivalent circuit model that fits both the α and β relaxation process[45] (see the ESI† for details of the fitting procedure). We emphasize that due to the employed measurement technique, the frequency range of both α and β processes can be covered without invoking time-temperature superposition, as it is often done in the literature. As processes with different temperature dependencies are observed, only such a broadband technique provides a proper data basis for a
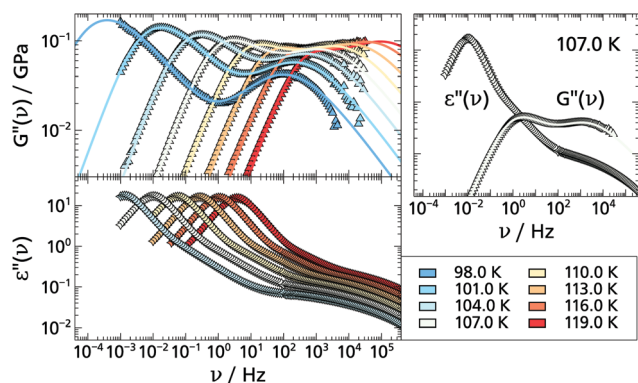
detailed comparison. In Fig. 2 (lower panel) the dielectric spectra at the same temperatures are shown. The dielectric spectrum is dominated by an intense low-temperature process (sometimes called the Debye process due to its mono-exponential nature), which is absent in the shear modulus spectra. The α and β process appear as distinct "bumps" on the high-frequency flank of the Debye process.

For a first comparison between TSD and shear data, Fig. 3 compares the time scales extracted from the shear modulus spectra to the α relaxation time scales of the TSD naphthalene data. The TSD α relaxation time scales were obtained by a common KWW fit to all TSD data shown in Fig. 1. The shift factor applied to make curves collapse provides an α relaxation time scale even for temperatures where only a small part of the curve is visible in the narrow time window of the TSD measurement. A near perfect match is found. Also shown are the dielectric Debye, α, and β relaxation times; as is often found, the shear α relaxation is faster than the dielectric relaxation (about a factor of $\sim$10).[46–49] The α time scale of the polar solvation data from ref. 26 shown for comparison clearly coincides with the dielectric α time scale, demonstrating that meso-scale structures responsible for the intense and slow Debye process are invisible to the local dielectric response.

A direct comparison of TSD and shear data in the time domain is shown in Fig. 4(a) giving rise to further evidence of agreement between the average local and the global mechanical response. To make a proper comparison, the complex shear data of Fig. 2 were interpolated to match the temperatures of the TSD measurements (see ESI† for details) and subsequently inverse Fourier transformed by using a variant of the Filon algorithm.[50] The match between TSD and shear data is within the experimental uncertainties. Thus, not only the time constants, but also the shape of the structural relaxation, as well as the relative strength ratio of the α to β processes as a function of temperature, agree for the local TSD and the macroscopic shear measurement techniques. This demonstrates that the Stokes
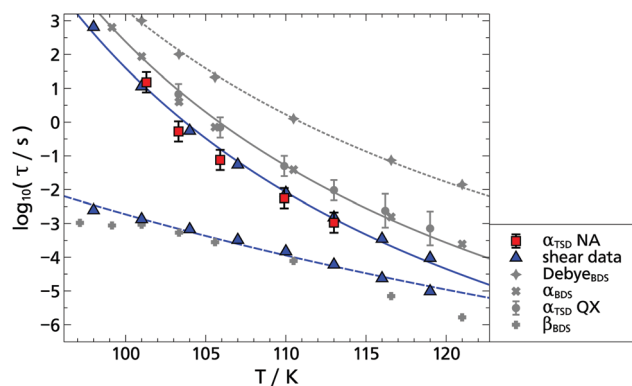

Fig. 2 Shear mechanical and dielectric spectra. Upper figure: imaginary part of the dynamic shear modulus of 1-propanol fitted by an electrical equivalent circuit model[45] (see also the ESI†). Lower figure: imaginary part of the dielectric spectra at the same temperatures as the shear mechanical data. The two responses are distinctly different, mainly due to the so-called intense Debye process, which is a strong single-exponential process characteristic of dielectric spectra of mono-alcohols. Right figure: a direct comparison between the shear mechanical and dielectric spectrum at a single temperature.

Fig. 3 Relaxation map of 1-propanol. The time scales extracted from the analysis of the nonpolar solvation data (red squares) and the shear modulus spectra (blue triangles) are shown to coincide within the experimental uncertainty. The polar solvation data (QX) from ref. 26 are added as well as those of the dielectric data. The polar solvation data and dielectric α time coincide with roughly the same temperature dependence as the shear data but almost a factor of 10 slower. Lines are guides to the eye.
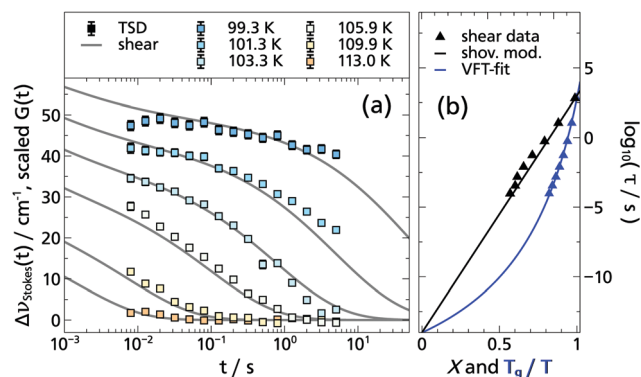
Fig. 4 (a) Comparison between $\Delta\nu_{\text{Stokes}}(t)$ and the inverse Fourier transformed, scaled shear modulus $G(t)$. $G(t)$ was interpolated to the TSD temperatures (*cf.* ESI†). Within the experimental uncertainty the time constants, as well as the shape of the structural relaxation, are identical for the two methods. Furthermore, the strength ratio of the α to β process is the same. This altogether demonstrates that NA probes a local dynamic shear response that is identical to the macroscopic response. (b) Test of the shoving model. The shear α time scale is shown as a function of inverse temperature scaled to T_g displaying the hallmark feature of viscous liquids: non-Arrhenius behavior (in blue). The same data points are plotted in black as a function of $X = \dfrac{G_\infty(T)\,T_g}{T\,G_\infty(T_g)}$. Plotted this way, the data points follow the model prediction (black line) with no free parameters (see text for details).

shift measured by the TSD technique using the nonpolar dye naphthalene is identical to the macroscopic shear modulus, except for a temperature-independent conversion factor which is 82 GPa^{-1} cm^{-1} in the case of 1-propanol. Although the TSD does not give directly the value of the local elastic modulus, it follows from this result that the macroscopic dynamic shear modulus is proportional to the average of the local dynamic shear modulus probed by the Stokes shift, with a proportionality constant that is temperature independent. In particular we find $G_{\infty,\text{macro}}(T) \propto G_{\infty,\text{local}}(T)$. These findings are consistent with the viscoelastic continuum model established for nonpolar fluorescence dye measurements,[28–31] which links the macroscopic dynamic shear modulus and the local Stokes shift response function. Fig. 4 comprises the first direct experimental proof of this connection.

The shoving model[51–53] for the non-Arrhenius temperature dependence of the structural relaxation time states that the activation energy is proportional to the local elastic high-frequency plateau modulus, $\Delta E \propto G_{\text{local}}$. The argument is the following: due to the anharmonicity of the intermolecular forces, it is energetically favorable for a flow event to take place when there is a slight local expansion of volume. The main contribution to the activation energy is the work needed to shove aside the surrounding liquid. Since the surrounding liquid behaves elastically on the picosecond time scale of a flow event, this work is proportional to the elastic modulus. Assuming a spherical region of expansion, the relevant elastic constant is G_∞. As mentioned in the introduction, it is very difficult to measure a local elastic shear modulus. Consequently, most tests of the shoving model have been performed with macroscopic measurements that in many cases, though

not always,[54] account for the non-Arrhenius temperature dependence of the relaxation time.

By extracting $G_\infty(T)$ from the fit curves of Fig. 2(a) and following a common procedure,[52,54,55] the model is tested for 1-propanol in Fig. 4(b). Here, the shear α relaxation time is plotted against the T_g/T in blue, displaying a clear non-Arrhenius behavior. The black data points are the same α time scales plotted against $X = \dfrac{G_\infty(T)\,T_g}{T\,G_\infty(T_g)}$. The variable X is $G_\infty(T)/T$ scaled to its value at T_g. Defining $\tau(T_g) = 1000$ s and a physically reasonable prefactor $\tau_0 = 10^{-14}$ s, the shoving model predicts the data points to follow the line $\log_{10}(\tau(T)) = 17X - 14$.[51] Although there are no free parameters, prediction and data match well.

4 Summary and conclusion

In summary, 1-propanol was investigated at temperatures slightly above T_g (up to $\sim 25\%$) using macroscopic rheology and the local TSD technique involving the nonpolar phosphorescence dye naphthalene. A comparison of TSD and shear data reveals that not only time constants, but also the shape of the structural relaxation and the strength ratio of the α to β process agree very well. This means that the local shear modulus can be measured with the TSD technique using the nonpolar dye naphthalene, thus settling the long-standing question of how nonpolar solvation data should be interpreted. From the perspective of the shoving model, these findings lends credibility to the procedure of using the macroscopic shear modulus when testing the model predictions – at least for 1-propanol. Clearly, more measurements of local dynamic elastic properties are desirable to elucidate the dynamics of glass-forming liquids. Meanwhile, it remains a challenge for theory to explain why the macroscopic elastic properties reflect simple averaging of local properties. This non-trivial result puts a constraint on future models of dynamic heterogeneities in glass-forming liquids. Our findings strongly suggest that the distribution of local dynamic shear moduli is – apart from a general temperature-dependent scaling factor – temperature-independent. In other words, all local dynamic shear moduli – and thus also the macroscopic dynamic shear modulus – change in the same way with temperature. This is highly non-trivial; thus recent extensive computer simulations show that this does not apply in general.[56]

Conflicts of interest

There are no conflicts to declare.

Acknowledgements

16540 | *Phys. Chem. Chem. Phys.*, 2021, **23**, 16537–16541

This journal is © the Owner Societies 2021

Notes and references

1 G. Tammann, *J. Soc. Glass Technol.*, 1925, **9**, 166–185.

2 W. Kauzmann, *Chem. Rev.*, 1948, **43**, 219–256.

3 J. H. Gibbs and E. A. DiMarzio, *J. Chem. Phys.*, 1958, **28**, 373–383.

4 M. Goldstein, *J. Chem. Phys.*, 1969, **51**, 3728–3739.

5 U. Bengtzelius, W. Gotze and A. Sjolander, *J. Phys. C: Solid State Phys.*, 1984, **17**, 5915–5934.

6 C. A. Angell, *J. Non-Cryst. Solids*, 1991, **131**, 13–31.

7 S. Sastry, P. G. Debenedetti and F. H. Stillinger, *Nature*, 1998, **393**, 554–557.

8 H. Sillescu, *J. Non-Cryst. Solids*, 1999, **243**, 81–108.

9 M. D. Ediger, *Annu. Rev. Phys. Chem.*, 2000, **51**, 99–128.

10 D. Chandler and J. P. Garrahan, *Annu. Rev. Phys. Chem.*, 2010, **61**, 191–217.

11 E. Lerner and E. Bouchbinder, *J. Chem. Phys.*, 2018, **148**, 214502.

12 J. C. Dyre, *Rev. Mod. Phys.*, 2006, **78**, 953–972.

13 V. Vitek and T. Egami, *Phys. Status Solidi B*, 1987, **144**, 145–156.

14 M. Tsamados, A. Tanguy, C. Goldenberg and J.-L. Barrat, *Phys. Rev. E: Stat., Nonlinear, Soft Matter Phys.*, 2009, **80**, 026112.

15 H. L. Peng, M. Z. Li, B. A. Sun and W. H. Wang, *J. Appl. Phys.*, 2012, **112**, 023516.

16 A. Marruzzo, W. Schirmacher, A. Fratalocchi and G. Ruocco, *Sci. Rep.*, 2013, **3**, 1407.

17 W. Schirmacher, G. Ruocco and V. Mazzone, *Phys. Rev. Lett.*, 2015, **115**, 015901.

18 B. Sun, Y. Hu, D. Wang, Z. Zhu, P. Wen, W. Wang, C. Liu and Y. Yang, *Acta Mater.*, 2016, **121**, 266–276.

19 A. A. Veldhorst and M. C. C. Ribeiro, *J. Chem. Phys.*, 2018, **148**, 193803.

20 P. Lunkenheimer, F. Humann, A. Loidl and K. Samwer, *J. Chem. Phys.*, 2020, **153**, 124507.

21 R. Richert, *J. Chem. Phys.*, 2000, **113**, 8404.

22 R. Richert, *Chem. Phys. Lett.*, 1992, **199**, 355–359.

23 R. Richert, F. Stickel, R. Fee and M. Maroncelli, *Chem. Phys. Lett.*, 1994, **229**, 302–308.

24 H. Wagner and R. Richert, *J. Non-Cryst. Solids*, 1998, **242**, 19–24.

25 D. Sauer, B. Schuster, M. Rosenstihl, S. Schneider, V. Talluto, T. Walther, T. Blochowicz, B. Stühn and M. Vogel, *J. Chem. Phys.*, 2014, **140**, 114503.

26 P. Weigl, D. Koestel, F. Pabst, J. P. Gabriel, T. Walther and T. Blochowicz, *Phys. Chem. Chem. Phys.*, 2019, **21**, 24778–24786.

27 H. Wendt and R. Richert, *J. Phys. Chem. A*, 1998, **102**, 5775–5781.

28 J. T. Fourkas, A. Benigno and M. Berg, *J. Chem. Phys.*, 1993, **99**, 8552–8558.

29 J. Ma, D. V. Bout and M. Berg, *J. Chem. Phys.*, 1995, **103**, 9146–9160.

30 M. Berg, *Chem. Phys. Lett.*, 1994, **228**, 317–322.

31 M. Berg, *J. Phys. Chem. A*, 1998, **102**, 17–30.

32 M. Z. Zgierski, *J. Chem. Phys.*, 1997, **107**, 7685–7689.

33 S. Kudoh, M. Takayanagi and M. Nakata, *J. Mol. Struct.*, 1999, **475**, 253–260.

34 R. Zhang and K. S. Schweizer, *J. Chem. Phys.*, 2017, **146**, 194906.

35 J. C. Berryman, *J. Acoust. Soc. Am.*, 1980, **68**, 1809–1819.

36 M. B. Isichenko, *Rev. Mod. Phys.*, 1992, **64**, 961–1043.

37 C. Gainaru, R. Figuli, T. Hecksher, B. Jakobsen, J. C. Dyre, M. Wilhelm and R. Böhmer, *Phys. Rev. Lett.*, 2014, **112**, 098301.

38 R. Böhmer, C. Gainaru and R. Richert, *Phys. Rep.*, 2014, **545**, 125–195.

39 V. Talluto, T. Blochowicz and T. Walther, *Appl. Phys. B: Lasers Opt.*, 2016, **122**, 122.

40 P. Weigl, V. Talluto, T. Walther and T. Blochowicz, *Z. Phys. Chem.*, 2018, **232**, 1017–1039.

41 T. Christensen and N. B. Olsen, *Rev. Sci. Instrum.*, 1995, **66**, 5019–5031.

42 B. Igarashi, T. Christensen, E. H. Larsen, N. B. Olsen, I. H. Pedersen, T. Rasmussen and J. C. Dyre, *Rev. Sci. Instrum.*, 2008, **79**, 045105.

43 B. Igarashi, T. Christensen, E. H. Larsen, N. B. Olsen, I. H. Pedersen, T. Rasmussen and J. C. Dyre, *Rev. Sci. Instrum.*, 2008, **79**, 045106.

44 T. Hecksher, N. B. Olsen, K. A. Nelson, J. C. Dyre and T. Christensen, *J. Chem. Phys.*, 2013, **138**, 12A543.

45 T. Hecksher, N. B. Olsen and J. C. Dyre, *J. Chem. Phys.*, 2017, **146**, 154504.

46 B. Jakobsen, K. Niss and N. B. Olsen, *J. Chem. Phys.*, 2005, **123**, 234511.

47 B. Jakobsen, C. Maggi, T. Christensen and J. C. Dyre, *J. Chem. Phys.*, 2008, **129**, 184502.

48 C. Gainaru, T. Hecksher, N. B. Olsen, R. Böhmer and J. C. Dyre, *J. Chem. Phys.*, 2012, **137**, 064508.

49 B. Jakobsen, T. Hecksher, T. Christensen, N. B. Olsen, J. C. Dyre and K. Niss, *J. Chem. Phys.*, 2012, **136**, 081102.

50 L. N. G. Filon, *Proc. R. Soc. Edinburgh*, 1930, **49**, 38–47.

51 J. C. Dyre, N. B. Olsen and T. Christensen, *Phys. Rev. B: Condens. Matter Mater. Phys.*, 1996, **53**, 2171–2174.

52 J. C. Dyre, T. Christensen and N. B. Olsen, *J. Non-Cryst. Solids*, 2006, **352**, 4635–4642.

53 S. Mirigian and K. S. Schweizer, *J. Chem. Phys.*, 2014, **140**, 194507.

54 T. Hecksher and J. C. Dyre, *J. Non-Cryst. Solids*, 2015, **407**, 14–22.

55 C. Maggi, B. Jakobsen, T. Christensen, N. B. Olsen and J. C. Dyre, *J. Phys. Chem. B*, 2008, **112**, 16320–16325.

56 G. Kapteijns, D. Richard, E. Bouchbinder, T. B. Schrøder, J. C. Dyre and E. Lerner, 2021, arXiv:2103.11404.